Selective bedload transport during the degradation of a well sorted graded sediment bed

Transport solide sélectif au cours de la dégradation d'un lit de sédiments calibrés bien triés

GARETH PENDER, *Professor, Department of Civil & Offshore, Engineering, Heriot-Watt University, Edinburgh, EH14 4AS, UK*

TREVOR B. HOEY, *Senior Lecturer, Department of Geography & Topographic, Science, University of Glasgow, Glasgow, UK*

CHRIS FULLER, *Research Assistant, Department of Civil Engineering, University of Glasgow, Glasgow G12 8LT, UK*

IAN K. McEWAN, *Senior Lecturer, Department of Engineering, University of Aberdeen, Aberdeen, UK*

ABSTRACT

The paper presents an analysis of the composition of bedload transport and changes to bed structure and topography during three graded sediment degradation experiments. The analysis suggests that variations in channel hydraulics and active layer composition alone may not explain the observed reductions in sediment transport. Further, the experiments appear to cover a crucial range of mean bed shear stresses for armouring studies, ranging between a condition of passive winnowing, to one of more active armour development in which the coarse grains play a role in determining bed structure. This indicates that the active layer concept, commonly applied in computer models of graded sediment transport, may be limited in its application.

RÉSUMÉ

On présente, dans cet article, la composition du transport solide, et les modifications de structure du lit et de topographie, au cours de trois expériences de dégradation d'éléments calibrés. L'analyse suggère que les variations de l'hydraulique du canal et de la composition de la couche active ne peuvent expliquer à elles seules les réductions de transport de sédiments observées. De plus, il semble que, dans les expériences, les contraintes tangentielles moyennes au fond couvrent une gamme de valeurs critiques pour les études de blindage entre une condition de vannage passif, et une autre de blindage plus actif dans lequel les sédiments grossiers jouent un rôle déterminant pour la structure du lit. Ceci indique que le concept de couche active, communément utilisé dans les modèles numériques de transport de sédiments calibrés, devrait être limité dans ses applications.

1. Introduction

Recent publications have discussed the bedload transport of graded sediment mixtures in field, flume and simulation studies (eg Parker, 1990; Wathen *et al.*, 1995; Wilcock and McArdell, 1993). Most of the studies have been in equilibrium or aggrading situations, and there has been less work on sediment transport composition during degradation. Understanding of this case is dominated by descriptions of the general decline in transport rate through time (Tait *et al.*, 1992; Proffitt and Sutherland, 1983) and of the dynamics of surface coarsening, (Sutherland, 1987). There have been few attempts to use bedload size distributions to inform about armouring processes, although Gomez (1994) illustrates the potential scope of this approach. In a recent study, Hassan and Church (2000) found that the development of surface structure during degradation exerted a significant influence upon bedload transport rates and grain sizes. Studies of degradation are important because they represent conditions, which occur during the low flow phases between floods. Consequently, the bed surface which results will determine bed stability and volume of sediment transported during subsequent flood events.

This paper presents observations from three bankfull flow experiments where a well sorted graded sediment bed was degraded. The results suggest that, for the conditions investigated, bedload composition, bed composition and bed structure are closely related, and so confirm the findings of Hassan and Church (2000). This may have implications for numerical models of graded sediment transport where the bed condition is normally simulated using an active layer (Hirano ,1971). This approach fails to take account of bed structure and could be a limiting factor in enabling reliable and accurate predictions of sediment movement in gravel bed rivers.

2. Experimental programme and conditions

The degradation experiments described were carried out as part of a larger series of experiments, which included the investigation of overbank flows and the bed response to sediment feed. Table 1 provides a summary of conditions employed in the experiments discussed here. They are numbered 1, 2 and 3 in order of decreasing initial energy gradient.

Experimental conditions were chosen to ensure negligible sus-

Table 1. Experimental Conditions

Experiment No.	Initial Energy Slope	Initial Depth (mm)	Initial Bed Roughness 'n'	Initial Bed Shear Stress (N/m^2)	Flow m^3/s
1	0.0026	150	0.016	3.82	0.117
2	0.0025	150	0.017	3.68	0.106
3	0.0022	150	0.016	3.24	0.107

Revision received October 25, 2000. Open for discussion till December 31, 2001.

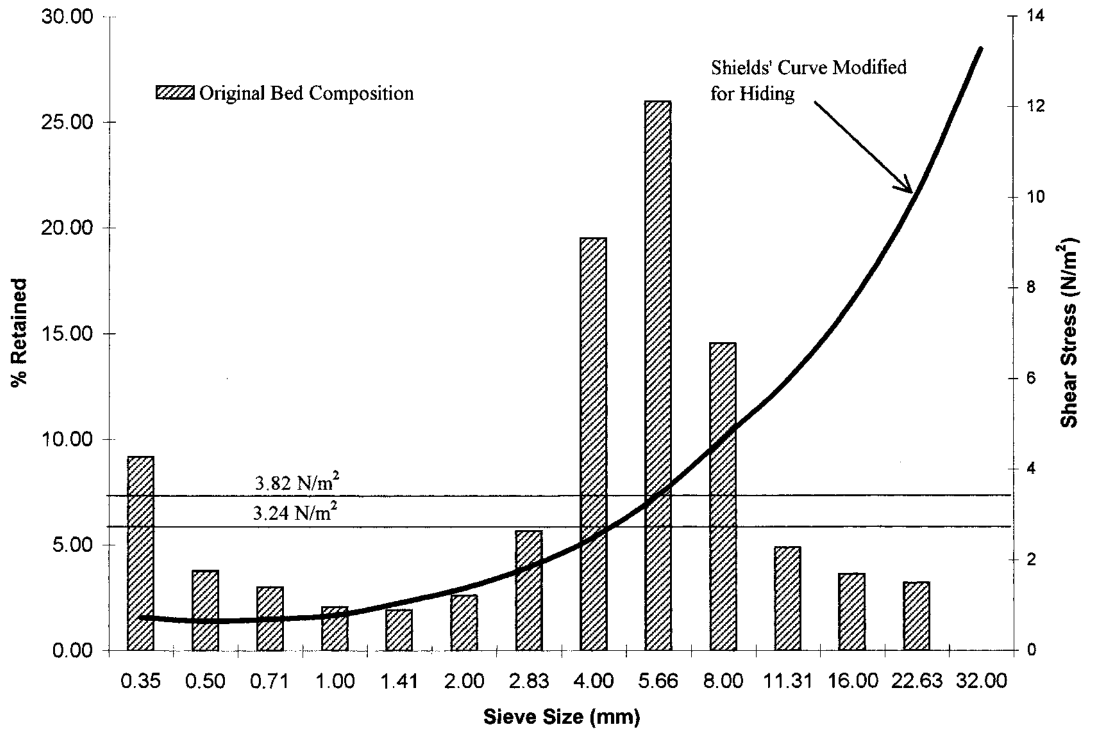

Fig. 1. Bed composition and size fraction mobility

pended load transport and selective bedload transport of the size fractions making up the bed material. It was therefore anticipated that the bed would armour progressively.

Fig. 1 gives an indication of the range of conditions covered. Critical conditions for each size fraction were estimated by modifying Shields' curve using the hiding function of White and Day (1982). The experimental shear stresses were obtained using measured values of energy gradient and uniform flow theory. The values presented have not been adjusted to account for the presence of the fixed walls as their influence on the applied bed shear stress is small. Based on White and Day's hiding function, and the estimates of applied shear stress one would expect size fractions less than 5.6 mm to be mobile and those greater to be immobile.

3. Experimental procedures

The flume is rectangular in section, 20 m long by 2.46 m wide by 0.6 m deep, and within the rectangular section a channel was cast in concrete, Fig. 2. The mobile bed was created by filling the central section with 170-mm–deep layer of graded sediment to create an initially trapezoidal channel.

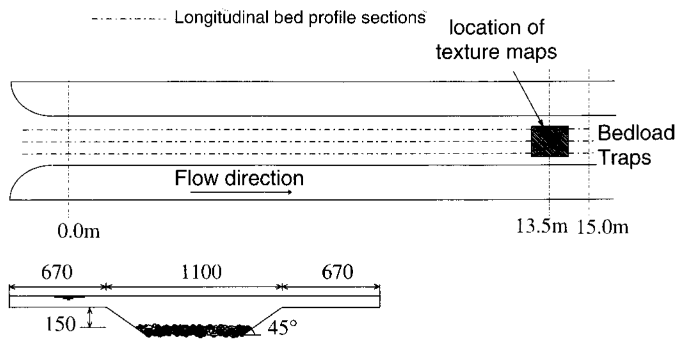

Fig. 2. Flume arrangement

In each experiment graded sediment was mechanically mixed to generate material with the distribution shown in Fig. 1 and the size distribution parameters given in Table 2. Regular sampling was used to ensure consistency of the mix composition along the channel. Statistical analysis of these samples indicated that there were no significant differences between the bed mixes for all experiments.

The graded sediment was placed in the central section of the flume and levelled relative to the channel flood plains to give a main channel bankfull depth of 150 mm. After a period of sub-threshold flow to remove unstable grains, the flow was increased to the experimental uniform flow value and data measurement started. Uniform flow was considered to exist when the water surface profile was parallel to the initial bed slope and the depth was equal to the bankfull condition along the length of the flume. Downstream boundary conditions were set using an adjustable tailgate. Although conditions were initially uniform and steady this procedure resulted in a small degree of unsteadiness and non-uniformity as no attempt was made to compensate for the progressive bed degradation and consequent depth variation along the channel by adjusting the water surface level from its bankfull condition.

Table 2. Changes in bed grading parameters; $\sigma_g=(d_{84}/d_{16})^{0.5}$

Experiment No.	Initial Energy Slope	Initial Depth (mm)	Initial Bed Roughness 'n'	Initial Bed Shear Stress (N/m²)	Flow m³/s
1	0.0026	150	0.016	3.82	0.117
2	0.0025	150	0.017	3.68	0.106
3	0.0022	150	0.016	3.24	0.107

Experiments were continued until the sediment transport rate had decreased to around 1% of its initial value. Depending on flow conditions this required between 80 and 100 hours.

4. Experimental measurements

Throughout the experiments periodic measurements were made of discharge, air and water temperature, longitudinal bed and water surface profiles, bedload transport rate and composition, and bed surface texture. Periodically, black and white photographs were taken of the bed surface.

Discharge measurement was achieved by measuring the pressure drop across a standard orifice plate using a pressure transducer. The sediment transport rate and bedload composition were determined at intervals from bedload samples collected in three traps placed transversely across the main channel at the same longitudinal position. Trap design and operation is described in Willetts, Pender and McEwan (1998). Their lateral dimensions ensured that bedload was trapped across the full width of the mobile bed. Longitudinal bed surface profiles were measured during the experiments at three locations; on the flume centreline and 180mm to either side. Measurements were obtained by traversing three lasers, attached to the instrument carriage, from the top to the bottom of the flume test section. The laser heads were submerged beneath the water surface. To minimise disturbance to the flow each laser was enclosed within a streamlined Perspex case. This had the additional benefit of protecting the lasers from splashing. The bed surface topography was also surveyed using a laser displacement sensor, during overnight periods when the flow was reduced to a sub-threshold level. A positioning system moved the sensor in a predetermined pattern both in the streamwise and transverse directions. This allowed the position of the sensor in the horizontal plane, and its vertical displacement from the bed surface to be determined simultaneously. The survey was performed over a grid of transverse and streamwise steps of 0.5 mm over an area of 256 x 256 mm, which was positioned, on the centreline of the inner channel approximately 1.5 m upstream of the bedload trap. At the beginning and end of each experiment the composition of the surface of the armoured bed was obtained using wax sampling (Marion, 1997), and these samples were then converted to an equivalent volumetric sample using the technique described by Fraccarollo and Marion (1997).

5. Results

Composition of the Armour Layer

The use of wax sampling as a means of determining armour layer composition possesses well documented limitations, Fripp and Diplas (1993). These, however, do not prevent the technique from identifying trends in bed composition during armouring. Final bed compositions from the wax sampling are compared with the initial bed composition in Fig. 3, where it can be seen that for each of the experiments the final bed possesses greater percentages of the coarsest (8-22mm) fractions than are present in the original bed. Relative to the initial bed there appears to be a reduction in the percentage of 5.66 mm, 4 mm and possibly 2.83 mm material in the final bed, whereas the material below 2 mm remains in approximately the same proportion. The consequence is that the grading parameters, given in Table 2, indicate the final bed to be coarser than the initial bed. In particular, it is notable that d_{84} increases most (by 64%) in Experiment 1 the steepest slope experiment, and by 46% and 37% at progressively flatter initial energy gradients. These increases are important given that this size is significant in determining flow resistance, Limerinos (1970).

Bedload

Fig. 4 shows plots of bedload transport rate against time for each of the experiments. The initial transport rate for Experiment 1 was measured as 61.65 g/s/m and is off the scale used in Fig. 4. This transport behaviour is typical of degradation experiments (Tait *et al*, 1992; Proffitt and Sutherland, 1993), showing; a rapid decline in transport rate (phase 1), followed by a period of low

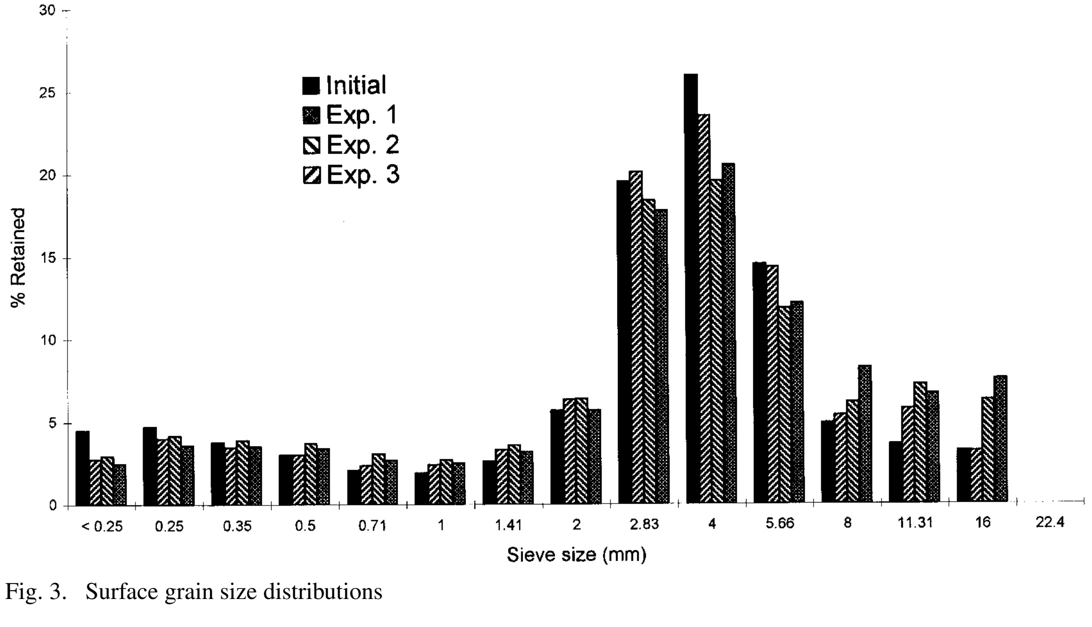

Fig. 3. Surface grain size distributions

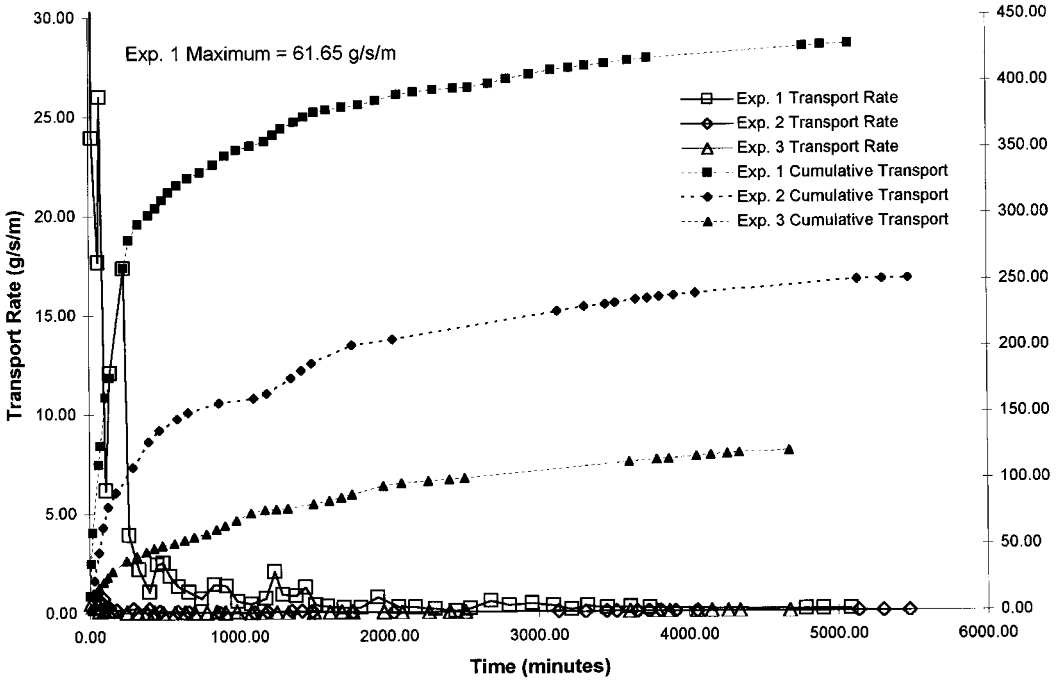

Fig. 4. Transport rates and cumulative mass transported

bedload transport activity (phase 2), decreasing to a marginal transport rate. In phase 1 the relatively loose newly constructed bed is eroded and undergoes restructuring. At the end of this phase the remaining sediment grains have been rearranged to provide a surface that has a significantly higher resistance to erosion than the original bed. Sediment transport from this water worked surface (phase 2) is sporadic in nature with some visual evidence that it takes the form of low amplitude bedload sheets, similar to those observed by Whiting et al.(1988). In degradation experiments stabilisation of the bed is generally thought to be a consequence of surface coarsening and a lowering of the energy gradient, however, as discussed later these are only two of the mechanisms that cause the bed to stabilise.

The difference in the transporting capacity of the flows can be seen more clearly in the cumulative transport plots also given on Fig. 4. It is clear from this that both the magnitude of the initial bedload transport rate and the total mass of sediment transported increases with the initial energy gradient, and hence the mean initial applied bed shear stress.

Composition of Bedload Transport

The composition of the bedload was determined throughout each experiment from the samples collected in the bedload traps. Changes in bedload size distributions through experiments reflect changing flow hydraulics and the availability of different sizes as armouring progresses. Fig. 5 illustrates the relative bedload trans-

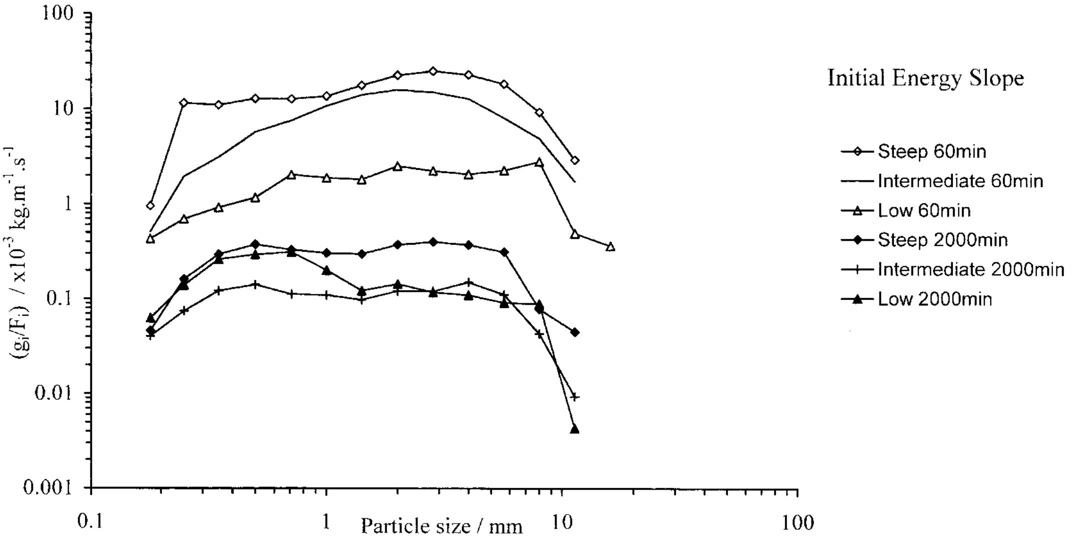

Fig. 5. Size fraction mobility at 60 minutes and 2000 minutes

port, g_i, of each size fraction for typical samples from phase one (60 minutes) and phase two (2000 minutes) of the experiments. Normalisation is by the surface grain size distributions, F_i, which indicate availability (initial surface samples are used to calculate F_i at 60 minutes, and end of experiment samples are used for 2000 minutes). In the early stages of all experiments the relative transport rates increase with grain size for sizes less than the median. The gradient of this trend differs between experiments, and is a maximum in Experiment 1 (Steep initial energy gradient). After 2000 minutes, Experiment 1 (Steep initial energy gradient) and Experiment 2 (Intermediate initial energy gradient) show similar patterns, with equal representation for sizes between 0.35 mm and 5.6 mm, but with both fine and coarse tails being under-represented. At the fine end, this suggests hiding of small particles beneath the coarser surface, and at the coarse end it suggests that larger particles are immobile within an armour layer. In Experiment 3 (Low initial energy gradient) mobility at 2000 minutes declines regularly for sizes between 0.71 and 11.6 mm, suggesting continued selective transport.

To assess the changes in bedload size distributions, the percentages in each size fraction were plotted against time on logarithmic axes. Approximately linear trends were observed in most cases, so ordinary least squares regression was used to fit lines of the form $\log(p_i)=a+b.\log(t)$, where p_i = % by mass in the size class, t = time (min) and a, b are regression constants. When plotted against grain size (Fig. 6) the gradients (b) reveal consistent trends between experiments. At the steepest slope, all sizes below the median reduce in abundance through the experiment, whereas larger sizes increase. As slope decreases, so the smaller sizes tend to increase in relative abundance, and the sizes greater than the median remain constant or decrease in significance. This may reflect the development of different types of armoured surface in the different experiments. It is suggested that in Experiment 3 (Low initial energy gradient) armouring occurs mainly by winnowing of the finer sizes leaving a coarse armour behind, whereas at steeper slopes where bedload transport is less marginal there is greater mobility of the larger sizes and hiding of finer sizes.

Analysis of the average of all bedload trap samples for phase 1 indicates that all fractions less than 2.00 mm behave in a similar manner. These fractions are therefore aggregated in the following analysis. The same approach has been adopted for fractions greater than 8 mm. Average bedload composition during the phase 1 decline in transport rate is shown in Fig. 7. Similar trends are observed for each experiment. Relative to their percentage in the initial bed, the sand size fractions (<2.00 mm) are under-represented in the bedload, the middle size fractions (2.00 mm, 2.83 mm and 4.00 mm) are over-represented, the 5.66 mm fraction is present in approximately the same percentage, and those greater than 8.00 mm are under-represented. Similar trends in the average bedload composition occur during phase 2.

Variations in Channel Bed Slope and Roughness

Table 3 provides a summary of the hydraulic conditions prevailing and channel changes occurring throughout the experiment, as expected bed degradation and armouring occurred, the extent of which increased with initial energy gradient. A consequence of this was a decrease in energy slope and an increase in bed roughness and a subsequent increase in flow depth (maximum 20 mm in Experiment 1). The depth of degradation roughly matches the increase in flow depth, resulting in flow conditions remaining close to uniform for the duration of the experiments. A typical laser bed profile measurement, from Experiment 1 is shown in Fig. 8(a). It can be seen that the bed is not planar, but possess irregularities caused by low amplitude bed forms, that form and then dissipate as they move downstream. These are similar in nature to the bedload sheets observed in Duck Creek by Whiting *et al.*, 1988, and exhibit similar patterns of longitudinal grain sorting.

Variations in average bed slope through time for Experiment 1 are shown in Fig. 8(b). It can be seen that in phase 2 the average energy gradient changes little as the bed degrades, similar results were obtained for Experiments 2 and 3. The final mean bed shear stress is invariably smaller than the initial one (Table 3). During the experiments, however, the shear stress may locally and temporally increase, although by very little.

Changes to Bed Topography

Figs 9(a) and (b) show photographs of the Experiment 1 (Steep initial energy gradient) bed taken at a distance of 15m, at elapsed times of 44 hours 39 minutes and 62 hours 27 minutes. The out-

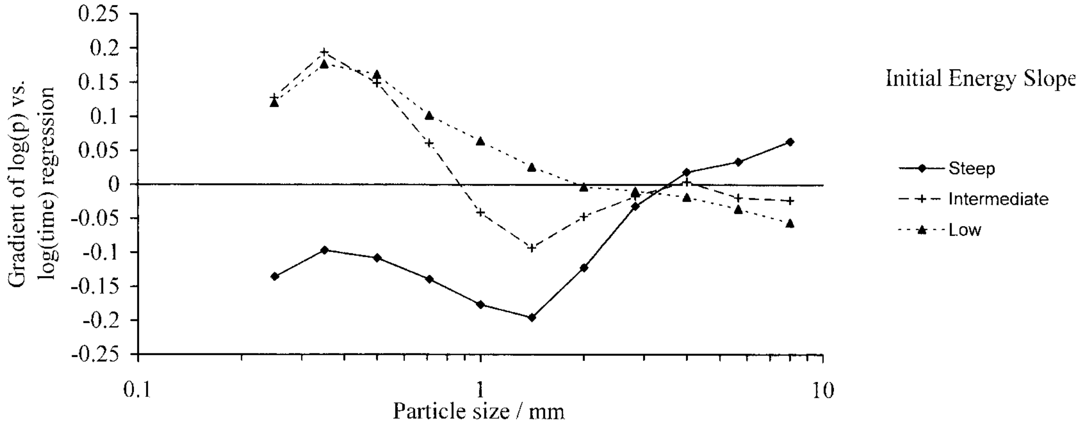

Fig. 6. Gradients of log-log regression of size fraction abundance vs. time, as a function of particle size

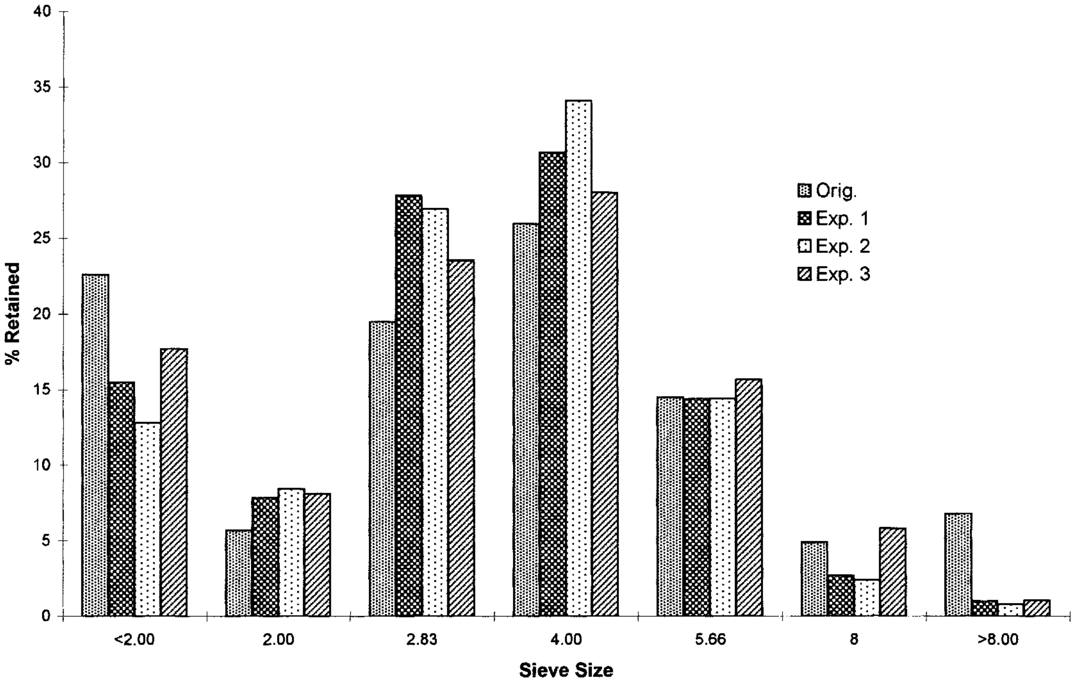

Fig. 7. Phase 1 bedload composition

Table 3 Final Hydraulic Conditions

Experiment	Final Average Energy Gradient	Final Average Flow Depth (mm)	Final Bed Roughness 'n'	Final Bed Shear Stress (N/m^2)	Experiment Duration (minutes)
1	0.0019	169	0.019	3.15	5134
2	0.0021	162	0.020	3.34	5555
3	0.0018	162	0.019	2.86	4800

lines of the larger grains at 62 hours 27 minutes are shown in Fig. 9(c); stable grains, which are also present at 44 hours 39 minutes, are shaded. Movement of grains between photographs is indicated by the arrows with the grain position at 44 hours 39 minutes shown by the dashed outline. From this it is evident that the population of coarse grains on the surface is increasing at this stage in the experiment, even though the bed load transport rate at this time is marginal, Fig. 4. In addition, it can be seen that a number of grains have changed position during the time period between photographs. Presumably these changes result in an increase in grain stability. The most obvious being grain , 'A' which has slid into a location where it is resting against grain 'B'. When viewed as a whole the grain outlines in Fig. 9(c) present a pattern similar to the stable diamond shaped grain patterns observed in the laboratory (Tait and Willetts,1991; Church, Hassan and Wolcott, 1998) and in the field (Church, Hassan and Wolcott, 1998; Kozlowski and Ergenzinger,1999). In these photographs the diamonds are less distinct than those presented by Tait and Willetts, but diagonal lines of larger grains are clearly visible suggesting that bed restructuring is an important element in determining the stability of the armoured surface for the initial energy gradient applied in Experiment 1.

Figs 10(a) and (b) show photographs of the bed for the same location in Experiment 3 (Low initial energy gradient), at 42 hours 41 minutes and 71 hours 40 minutes. Again changes in the bed surface structure are apparent at this low bedload transport stage in the experiment. However, highlighting the coarse grains in this case, Fig. 10(c) shows that there are fewer coarse grains in the

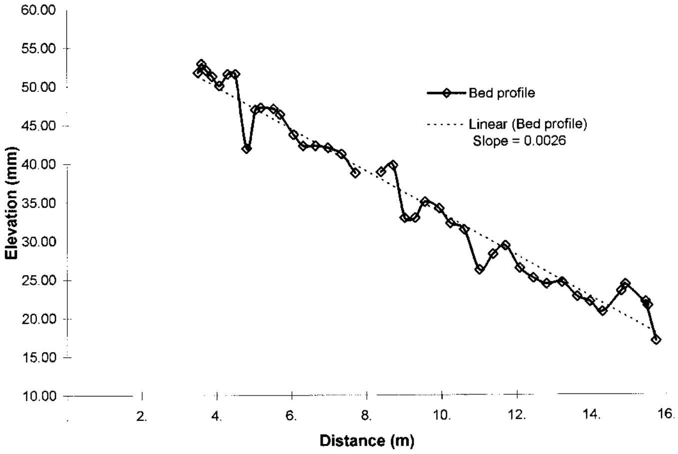

Fig. 8(a). Typical laser profile of mobile bed

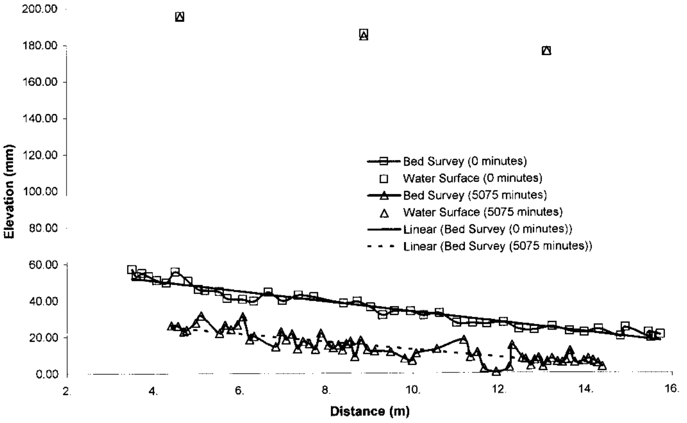

Fig. 8(b). Bed slope changes during Experiment 1

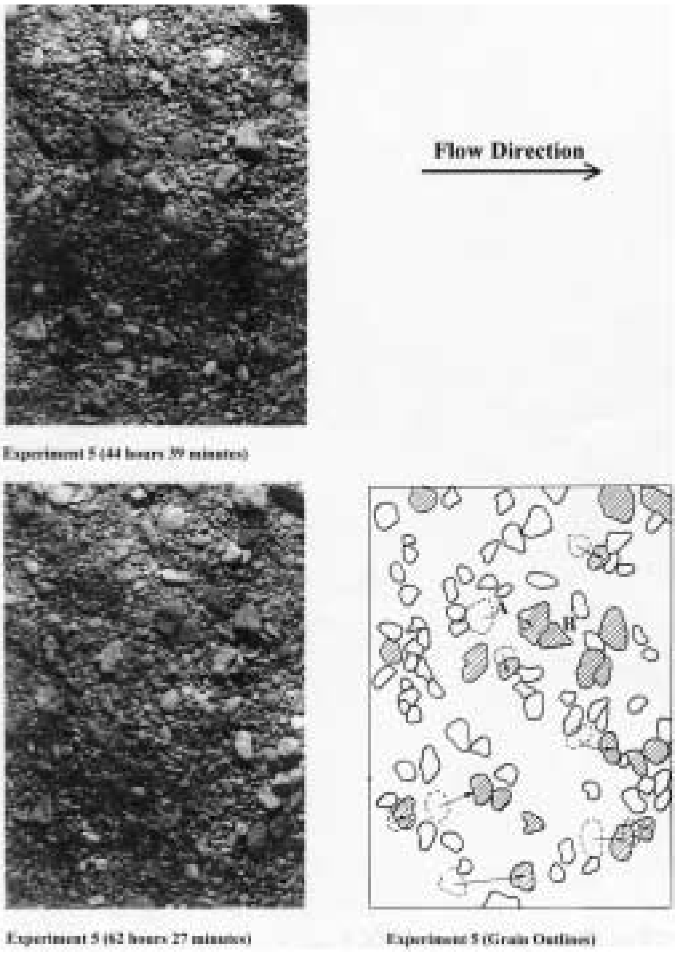

Fig. 9. Bed photographs Experiment 1

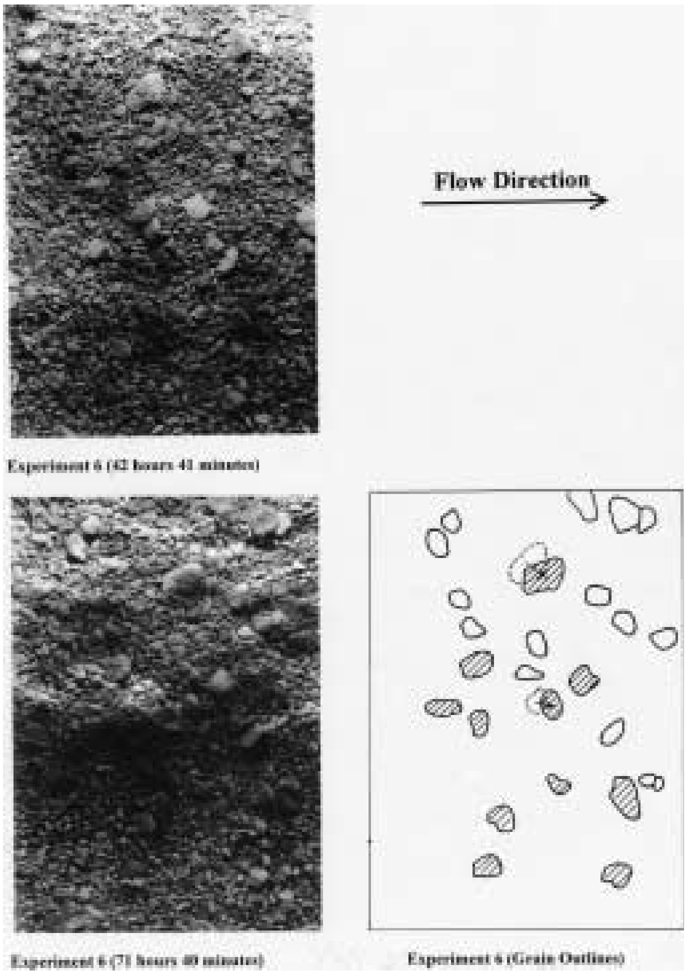

Fig. 10. Bed photographs Experiment 3

final bed surface for this applied shear stress. In addition, the interconnected diagonal grain structures observed for the steeper initial energy gradient do not appear to be present here. This is consistent with the observation made above that at the lower initial energy gradient the coarse grains play a less active role in armour development and are therefore less likely to form an interconnected structure.

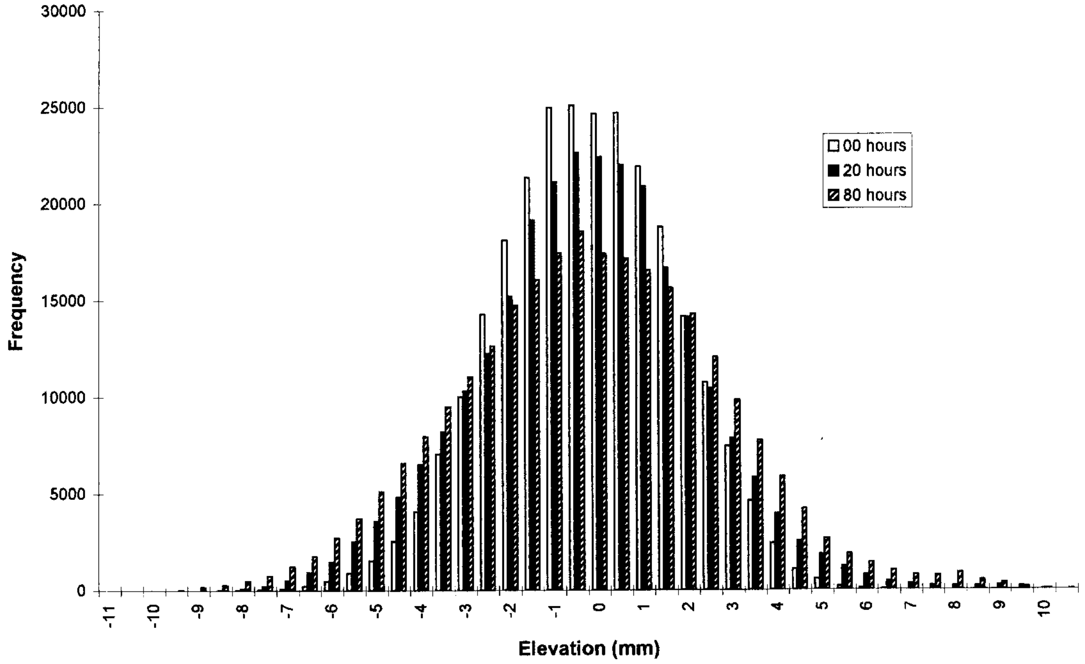

Fig. 11. Bed elevation frequencies Experiment 3

6. Discussion

Bedload Composition

The observation that sizes greater than 5.66 mm are under-represented in the bedload can be explained by Fig. 2, where it is indicated that the applied shear stress is less than the critical value for this size of material. The apparent behaviour of the fractions less than 2.00mm is more surprising. They are present in the bedload, but in a smaller percentage than they are present in the bed material at both the start and the end of the experiments. This can be partially explained due to sheltering effects. However, the results indicate that the degree of sheltering obtained during degradation is greater than suggested by the marginal increase in critical shear stress predicted by the hiding function, Fig. 2. The observation is similar to that made by Wilcock and Southard (1989) for the initial transport rates from their equilibrium experiments where hydraulic conditions were closest to incipient motion. Identifying the reason for this requires further investigation, however, it could be that the smaller size fractions move down into the interstices between the larger grains during bed restructuring in phase 1.

Bedload transport rate and bed structure

The significant changes in bedload transport rate observed during these experiments are due to a combination of changes in channel hydraulics, bed composition, bed structure and bed topography. Although an appreciable decrease in the shear stress is observed at the end of the experiments (between 12% and 14%), variations in channel hydraulics alone may not explain the observed reduction in bedload transport. As previously discussed all experiments result in a final bed, which is coarser than the original. The variations shown in Fig. 3 indicate that changes in bed surface composition are relatively slight and will account for only a small plan area of the bed. This suggests that the coarse grains act to stabilise a significantly larger area of the bed than their plan area suggests. Hassan and Church (2000) calculated that between 17 and 47% of the shear stress after degradation is due to structure, with nearly all of the remainder being borne by the grains. In Experiment 1 there is evidence to support Tait and Willetts (1991) observation that this is due to the formation of coarse grain structures that act to protect relatively finer areas of the bed. However, in Experiment 3 a stable bed has been obtained without any visual evidence of the formation of these structures. This is consistent with the observation made above that in Experiment 3 the coarse grains play a less active role in armour development and are therefore less likely to form an interconnected structure.

Analysis of the laser texture data undertaken by Marion, McEwan and Tait (1997) suggests that this may be due to changes in bed topography. The most fundamental method of analysing this is to count the frequency of measurements above and below mean bed level in intervals of elevation. Fig. 11 shows the change in these frequency diagrams throughout Experiment 3. In general, one observes a spreading of the frequency plots as time progresses. This process continues well into phase two of the degradation process and is consistent with the increasing number of large grains seen in Figs 9(a) and (b). These bed topography changes result in a marginal change in hydraulic roughness and a 12% reduction in average bed shear stress as indicated in Table 3. These are, therefore, not sufficient to explain the observed reduction in transport rate. This supports Tait and Willetts (1991) thesis, reinforced by Hassan and Church (2000), that describing changes in bed surface texture and topography is an essential prerequisite to predicting the behaviour of gravel bed rivers.

7. Conclusions

The three experiments described above are all occurring under marginal transport conditions (i.e. shear stress is only above threshold for part of the grain size distribution). The experiments show similar behaviour through time and appear at a qualitative level to develop armouring in similar ways. However, detailed inspection of the nature of the transported sediment and the characteristics of the armoured bed suggests that different modes of behaviour are occurring at different initial energy gradients rather than different intensities of the same basic armouring process. It suggests that the experiments cover a crucial range of conditions for armouring studies, ranging from a condition of passive winnowing, Sutherland (1987), to one of more active armour development in which the coarser grains play an active role in determining bed structure.

For the experiments reported, changes in bedload transport may not be explained by variations in mean flow conditions and bed composition alone. It is therefore thought that the measured changes in bedload transport are a result of a combination of changes in channel hydraulics, bed structure and topography. Each of these mechanisms may exist in both experiments, however the photographic evidence suggests that structure is important in the higher shear stress experiment, whereas the interaction of bed topography and channel hydraulics would appear to be a significant factor in the lower shear stress experiment.

These findings have implications for numerical models of graded sediment transport where the bed condition is normally simulated using an active layer, e.g. Hirano (1971). This approach fails to take account of bed structure and topography, which could be a limiting factor in enabling reliable and accurate predictions of sediment movement in gravel bed rivers, especially near to incipient motion conditions.

Acknowledgements

The research is sponsored by the U.K. Engineering and Physical Sciences Research Council, and is being undertaken by the Universities of Aberdeen and Glasgow. HR Wallingford is thanked for use of the experimental facility and technical support. Dr. Andrea Marion provided the surface grain size data.

References

Church, M., Hassan, M.A. and Wolcott, J.F. (1998) Stabilizing self-organized structures in gravel-bed stream channels: field and experimental observations. *Water Resources Re-*

search 34(11), 3169-3179.

FRIPP, J.B. and DIPLAS, P. (1993) Surface sampling in gravel streams. *J. Hyd. Eng.*, ASCE, 119(4), 473 - 490.

GOMEZ, B. (1994). Effects of particle shape and mobility on stable armor development. *Water Resources Research*, 30, 2229-2239.

HASSAN, M.A. and CHURCH, M. (2000) Experiments on surface structure and partial sediment transport on a gravel bed. *Water Resources Research*, 36(7), 1885-1895.

HIRANO, M. (1971) River bed degradation with armouring. *Proc. Japanese Soc. of Civil Engineers*, 195, 55-65.

KOZLOWSKI, B. and ERGENZINGER, P. (1999) Ring Structures – A Specific New Cluster Type in Steep Mountain Torrents. *Proc. XXVIIIth IAHR Congress*, Graz, Austria (22-27) August, CD-ROM.

LIMERINOS, J.T. (1970) Determination of Manning coefficient from measured bed roughness in natural channels. Water Supply. *US Geological Survey*, Paper 1898-B.

MARION, A. (1996). Equilibrium bed material composition for well-graded sediment mixtures in a compound channel. *Report SR474*, HR Wallingford.

MARION, A., MCEWAN, I. and TAIT, S. (1997) On the competitive effects of particle re-arrangement and vertical sorting, *Proc. XXVII IAHR Congress*, San Francisco, USA, pp 1493-1498.

MARION, A. and FRACCAROLLO, L. (1997). A new conversion model for areal sampling of fluvial sediments. *Journal of Hydraulic Engineering,* Vol.123, No. 12, December, pp 1148-1151.

PARKER, G. (1990). Surface-based bedload transport relation for gravel rivers. *Journal of Hydraulic Research*, 28, 417-436.

PROFFITT, G.T., and SUTHERLAND, A.J. (1983). Transport of non-uniform sediment. *Journal of Hydraulic Research*, 21, 33-43.

SUTHERLAND, A.J. (1987) Static armour layers by selective erosion. *Sediment Transport in Gravel-Bed Rivers*, C.R. Thorne et al., Wiley, Chichester, 243-60.

TAIT, S.J. and WILLETTS B.B (1991) Characterisation of armoured bed surfaces, *Proc. Int. Grain Sorting Seminar*, Zurich.

TAIT, S.J., WILLETTS, B., MAIZELS, J.K.(1992). Laboratory observations of bed armouring and changes in bedload composition. *Dynamics of Gravel Bed Rivers*, P.Billi *et al.*, Wiley, Chichester, 205-25.

WATHEN, S.J., FERGUSON, R.I., HOEY, T.B., and WERRITTY, A. (1995). Unequal mobility of gravel and sand in weakly bimodal river sediments. *Water Resources Research*, 31, 2087-2096.

WHITE, W. R. and DAY, T. J. ((ed.)). Transport of graded gravel bed material. *Gravel Bed Rivers*, Hey R. D. *et al.*, John Wiley, 1982, 181 - 213.

WHITING, P.J., DEITRICH, W. E., LEOPOLD, L. B., DRAKE, T. G., and SHREVE, R. L. (1988) Bedload sheets in heterogeneous sediment. *Geology*, The Geological Society of America, 16(2), 105-108.

WILCOCK, P.R. and SOUTHHARD, J.B. (1989) Bed load transport of mixed size sediment: fractional transport rates, bed forms, and the development of a coarse bed surface layer. *Water Resources Research*, 25 (7), 1629 - 1641, July.

WILCOCK, P.R., and MCARDELL, B.W. (1993). Surface based fractional rates: mobilization thresholds and partial transport of a sand-gravel sediment. *Water Resources Research*, 29, 1297-1312.

WILLETTS, B.B., PENDER, G. and MCEWAN, I.K. (1998) Transport of poorly sorted sediments in high stage flows, *Proc. Instn Civ. Engrs Wat. Marit. and Energy*, Vol. 130, No. 4, Dec 1998.